

Anisotropy induced large exchange bias behavior in ball milled Ni–Co–Mn–Sb alloys

Nayak, Ajaya K.; Sahoo, Roshnee; Suresh, K. G.; Nigam, A. K.; Chen, X.; Ramanujan, R. V.

2011

Nayak, A. K., Sahoo, R., Suresh, K. G., Nigam, A. K., Chen, X., & Ramanujan, R. V. (2011). Anisotropy induced large exchange bias behavior in ball milled Ni–Co–Mn–Sb alloys. *Applied physics letters*, 98(23), 232502-.

<https://hdl.handle.net/10356/105794>

<https://doi.org/10.1063/1.3597305>

© 2011 American Institute of Physics. This paper was published in *Applied Physics Letters* and is made available as an electronic reprint (preprint) with permission of American Institute of Physics. The paper can be found at the following official DOI: [<http://dx.doi.org/10.1063/1.3597305>]. One print or electronic copy may be made for personal use only. Systematic or multiple reproduction, distribution to multiple locations via electronic or other means, duplication of any material in this paper for a fee or for commercial purposes, or modification of the content of the paper is prohibited and is subject to penalties under law.

Downloaded on 03 Oct 2023 02:34:07 SGT

Anisotropy induced large exchange bias behavior in ball milled Ni–Co–Mn–Sb alloys

Ajaya K. Nayak, Roshnee Sahoo, K. G. Suresh, A. K. Nigam, X. Chen, and R. V. Ramanujan

Citation: *Applied Physics Letters* **98**, 232502 (2011); doi: 10.1063/1.3597305

View online: <http://dx.doi.org/10.1063/1.3597305>

View Table of Contents: <http://scitation.aip.org/content/aip/journal/apl/98/23?ver=pdfcov>

Published by the *AIP Publishing*

Articles you may be interested in

[Phase coexistence induced by cooling across the first order transition in Ni–Co–Mn–Sb shape memory alloy](#)
J. Appl. Phys. **108**, 063915 (2010); 10.1063/1.3483951

[Irreversibility of field-induced magnetostructural transition in NiCoMnSb shape memory alloy revealed by magnetization, transport and heat capacity studies](#)
Appl. Phys. Lett. **96**, 112503 (2010); 10.1063/1.3365181

[Pressure induced magnetic and magnetocaloric properties in NiCoMnSb Heusler alloy](#)
J. Appl. Phys. **106**, 053901 (2009); 10.1063/1.3208064

[Exchange bias behavior in Ni–Mn–Sb Heusler alloys](#)
Appl. Phys. Lett. **91**, 072510 (2007); 10.1063/1.2772233

[Microstructure and exchange coupling in nanocrystalline Nd₂\(FeCo\)₁₄B/FeCo particles produced by spark erosion](#)
Appl. Phys. Lett. **86**, 122507 (2005); 10.1063/1.1890474



ZABER

Automate your set-up with
Miniature Linear Actuators

Affordable. Built-in controllers.
Easy to set up. Simple to use.

www.zaber.com



Anisotropy induced large exchange bias behavior in ball milled Ni-Co-Mn-Sb alloys

Ajaya K. Nayak,¹ Roshnee Sahoo,¹ K. G. Suresh,^{1,a)} A. K. Nigam,² X. Chen,³ and R. V. Ramanujan³

¹Department of Physics, Indian Institute of Technology Bombay, Mumbai 400076, India

²Tata Institute of Fundamental Research, Homi Bhabha Road, Mumbai 400005, India

³School of Materials Science and Engineering, Nanyang Technological University, Singapore 639798

(Received 13 March 2011; accepted 16 May 2011; published online 6 June 2011)

We report the effect of decrease in the grain size on the structural, magnetic and exchange bias (EB) behavior in ball milled $\text{Ni}_{50-x}\text{Co}_x\text{Mn}_{38}\text{Sb}_{12}$ ($x=0$ and 5) Heusler alloys. The existence of a wide range of grain sizes in the ball milled samples results in dramatic changes in the structural and magnetic properties. For $x=0$, a large EB field of 3.2 kOe is observed in the ball milled sample, compared to a value of 245 Oe of the bulk sample. This increase is attributed to the enhanced exchange coupling between the soft and hard magnetic particles. © 2011 American Institute of Physics. [doi:10.1063/1.3597305]

In the last decade, Ni-Mn-X (X=Ga, Sn, In, and Sb) based ferromagnetic (FM) shape memory alloys have received significant research interest due to their potential applications in various fields. Depending upon the Mn/X ratio, these alloys undergo austenite to martensite structural transition resulting in different magnetic states in the two phases due to strong magneto-structural coupling. As a consequence of this transition these alloys exhibit large field induced shape memory effect,^{1,2} giant magnetocaloric effect,³ large magnetoresistance,^{4,5} exchange bias (EB) behavior,^{6,7} etc. The alloy composition, external parameters like magnetic field, hydrostatic pressure and repeated structural change are known to stabilize one phase at the expense of the other.^{4,8,9}

The theoretical study by Meng *et al.*¹⁰ shows that the nucleation barrier and the critical grain size for phase transformations in nanosized crystals are predominantly dependent on the strain energy, interphase boundary energy and the grain size. The effect of reduction in grain size by ball milling on the structural properties of these alloys has been studied in Ni-Mn-Ga alloy, which shows nonexistence of structural transition in the system due to decrease in the grain sizes.^{11,12} This implies that the austenite grains must possess some critical size to undergo the structural transition. However, the critical grain size may be different for different systems. The reduction in the strength of the FM state with very short milling time is reported in Ni-Mn-Sn alloy.¹³ In this letter, we report the effect of grain size reduction, obtained by high energy ball milling of arc melted $\text{Ni}_{50-x}\text{Co}_x\text{Mn}_{38}\text{Sb}_{12}$ ($x=0$ and 5) alloys, on the structural, magnetic and EB behavior.

Polycrystalline ingots of compositions $\text{Ni}_{50-x}\text{Co}_x\text{Mn}_{38}\text{Sb}_{12}$ ($x=0$ and 5) were prepared by arc melting the stoichiometric amounts of Ni, Co, Mn, and Sb of at least 99.99% purity in high pure argon atmosphere and were subsequently annealed in evacuated quartz tubes at 850 °C for 24 h. About 3% extra manganese was added to compensate the weight loss and the final weight loss was always less than 1% of the initial weight. The annealed samples were subjected to high energy ball milling to get the reduced particle size. The milling process used tungsten carbide balls

with 200 rpm in N_2 atmosphere for 15 h. The structural characterization was carried out by powder x-ray diffractograms (XRDs) using $\text{Cu } K\alpha$ radiation. The scanning electron microscopy (SEM) measurements have been carried out using an ESEM-FEI quanta 200 model. The magnetization measurements were carried out using a vibrating sample magnetometer attached to a Physical Property Measurement System (Quantum Design, PPMS-6500)/superconducting quantum interface device magnetometer (Quantum Design).

The room temperature XRD patterns for the ball milled $\text{Ni}_{50-x}\text{Co}_x\text{Mn}_{38}\text{Sb}_{12}$ ($x=0$ and 5) samples are shown in Fig. 1. The existence of (220) L_{21} peak and the absence of (111) and (200) superlattice peaks signify the disordered austenite phase at room temperature. The bulk alloy with $x=5$ exhibits austenite phase, whereas the alloy with $x=0$ exhibits martensite phase at room temperature.¹⁴ Therefore, it is clear that in the alloy with $x=0$ the ball milling process has transformed the low symmetry/ordered martensite phase to the higher symmetry/ordered austenite phase. This type of phase transition during the milling process has also been observed in Ni-Mn-Ga (Refs. 11 and 13) and ZrO_2 .¹⁵ This implies that the increase in the strain energy and interfacial boundary energy due to the decrease in grain size brought about by ball

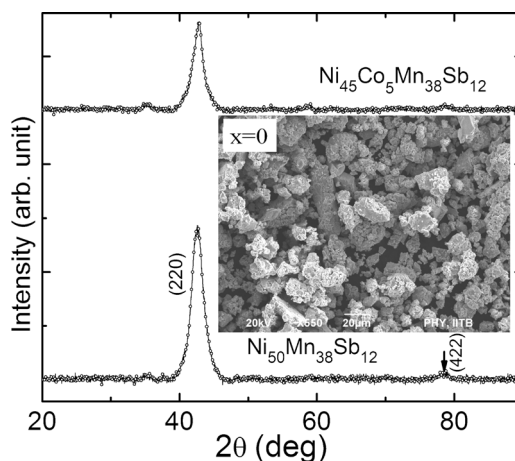


FIG. 1. Room temperature XRD patterns for ball milled $\text{Ni}_{50-x}\text{Co}_x\text{Mn}_{38}\text{Sb}_{12}$ ($x=0$ and 5) alloys. The inset shows the SEM image for $x=0$ with scale of 20 μm .

^{a)}Electronic mail: suresh@phy.iitb.ac.in.

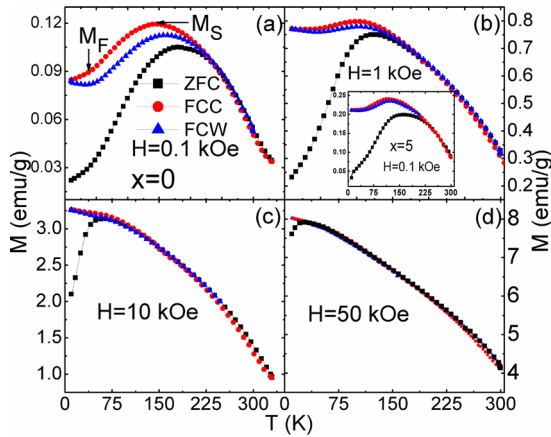


FIG. 2. (Color online) ZFC (square), FCC (circle), and FCW (triangle) thermomagnetic $[M(T)]$ curves for $x=0$ taken in different measuring fields. Inset of (b) shows the $M(T)$ for $x=5$ measured in 0.1 Oe field.

milling completely destabilize the martensite phase. The SEM micrograph for $x=0$ is shown in inset of Fig. 1, which shows particles with sizes ranging from 1 to 50 μm .

Figure 2 shows the thermo magnetic, $M(T)$, curves for the ball milled $x=0$ sample measured in zero field cooled (ZFC), field cooled cooling (FCC) and field cooled warming (FCW) modes with different measuring fields. The $M(T)$ curves measured in 0.1 kOe [Fig. 2(a)] reveals the martensitic transition, which is accompanied by the hysteresis between the FCC and FCW data at around 150 K. It is to be noted that the martensitic transition in the bulk alloy occurs at around 335 K.¹⁴ This implies that the decrease in the grain size destabilizes the martensite phase. This is consistent with the observations of a decrease in the strength of the martensitic transition in ball milled Ni–Mn–Sn particles.¹³ The absence of the martensitic transition in micron sized (ball milled) Ni–Mn–Ga particles¹² and nanosized ball milled Ni–Mn–Ga powder particles¹¹ also support the present data. The broad nature of the martensitic transition as well as the magnetic order-disorder transition is consistent with the wide distribution of the grain sizes in the sample. The $M(T)$ curve for $x=5$ shows almost zero thermal hysteresis between the FCC and FCW modes [inset of Fig. 2(b)], indicating only a very weak martensitic transition, in contrast to the well defined martensitic transition around 260 K in the bulk sample.¹⁴

Another interesting property (Fig. 2) is the existence of a large separation between the ZFC and FCW curves at low temperatures. This irreversibility exists for applied fields as large as 50 kOe (Fig. 2(a)–2(d)). This suggests that there is an additional contribution for the increased thermomagnetic irreversibility. The development of large magnetic anisotropy due to decrease in the grain size and the formation of non circular grain size in the ball milled sample must be responsible for the enhanced irreversibility. Such an increase in the magnetic anisotropy has also been observed in other ball milled samples as well.^{16,17} The decrease in FM strength in the ball milled sample for both $x=0$ and 5 is identical to that seen in ball milled Ni–Mn–Sn sample.¹³

To further study the origin of the large thermomagnetic irreversibility observed in Fig. 2, we have measured the field cooled magnetic isotherms, $M(H)$, at different temperatures (Fig. 3). Prior to the measurement a field of 50 kOe was applied at room temperature and the sample subsequently cooled to the desired temperature, where the measurement

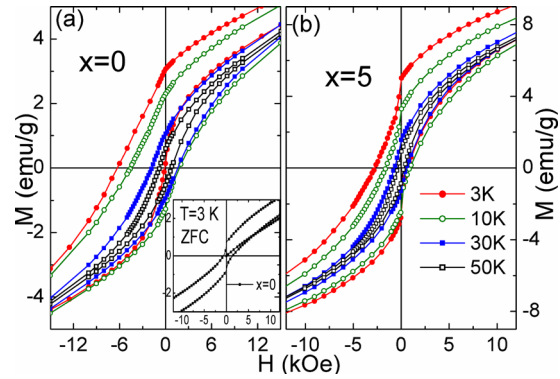


FIG. 3. (Color online) $M(H)$ isotherms measured at different temperatures after field cooling the sample in 50 kOe for (a) $x=0$ and (b) $x=5$. The inset of (a) shows the ZFC $M(H)$ loop measured at 5 K for $x=0$.

was conducted in ± 50 kOe range. For better clarity, the $M(H)$ loops are shown only for the range of ± 15 kOe for $x=0$ and ± 12 kOe for $x=5$. In both the samples the field cooled $M(H)$ isotherms shift drastically to negative fields. Though a similar trend was seen in the bulk alloys also,¹⁴ the shift is much larger in the present case. The most important fact is that the field cooled $M(H)$ isotherms show double shifted loops having two coercive fields, which vanish for temperatures above 40 K. The ZFC $M(H)$ loop at 3 K [inset of Fig. 3(a)] also shows the double shifted loop. It is to be mentioned here that in the bulk alloys of the same compositions, though the ZFC data showed the double shifted loop, it was absent in the FC data.¹⁴ In general, the double shifted $M-H$ behavior has been observed in systems consisting of two magnetic phases possessing different coercive fields and hence different magnetic anisotropies.^{18–21} In such materials, exchange coupling between hard and soft FM layers is known to be present and the magnetization of the soft layer changes due to the hard layer. In the present case the ball milled samples consist of different particle sizes. The larger grain size particles act as a magnetically soft medium (less magnetic anisotropy), whereas the smaller grain size particles act as the magnetically hard (large magnetic anisotropy) phase. In low fields, the magnetic response mainly results from the soft FM layer, which gives rise to a sudden decrease/increase in the magnetization. It is of importance to note that in the case of bulk samples the low temperature ZFC $M(H)$ isotherms showed almost zero coercive field and zero hysteresis.¹⁴ Therefore, the existence of large hysteresis and nonzero coercive field in the ZFC loop of the ball milled samples supports our conjecture of enhanced magnetic anisotropy in the ball milled samples. The shift in the field cooled loops along the field axis is mainly due to the exchange interaction between the soft and hard magnetic particles, in addition to the usual nominal exchange bias associated with the FM and AFM components of the bulk alloys.

The variations in exchange bias field (H_{EB}) and coercive field (H_C) with temperature for $x=0$ and 5 are shown in Fig. 4. A maximum H_{EB} of 3.2 kOe for $x=0$ and 1.05 kOe for $x=5$ have been obtained at 3 K. It may be recalled here that the maximum H_{EB} of 245 Oe for $x=0$ and 480 Oe for $x=5$ were obtained in the bulk samples.¹⁴ The large increase in EB behavior in the ball milled samples is due to the mixture hard and soft FM particles. Increase in EB field is also reported in Ni–Mn–Sn alloys with very short time ball milling.¹³ A similar large EB behavior has been observed in a

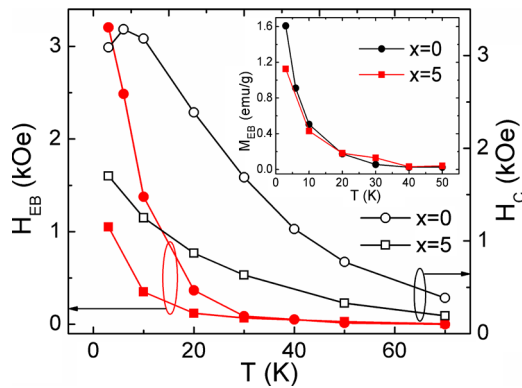


FIG. 4. (Color online) Temperature dependence of H_{EB} (closed symbols) and H_C (open symbols) for $x=0$ (circle) and $x=5$ (square). The inset shows temperature dependent of M_{EB} .

CoCr/CoPtCrB bilayer system consisting of soft and hard magnetic layers and the shift in $M(H)$ loop was attributed to exchange interactions between the hard and soft FM layers.²¹ A similar exchange interaction may exist in the present ball milled samples, giving rise to a large shift in the $M(H)$ loop. The temperature dependence of M_{EB} (shift in zero field magnetization along the magnetization axis) is shown in the inset of Fig. 4. M_{EB} is calculated as $M_{EB}=(M_1+M_2)/2$, where M_1 and M_2 are the lower and upper cutoff magnetization at zero field. It is observed that the M_{EB} versus T curves follow the same behavior as the H_{EB} versus T curves.

Figure 5 shows the field dependence of magnetization measured at 3 K after cooling the sample to the desired temperature in different fields (H_{FC}). The increase in the remanent magnetization as well as coercive fields with higher cooling field is due to an increase in the FM component at higher fields. Importantly, the signature of the double shifted loop increases with increase in the cooling field. At lower cooling fields the hard FM particles are not saturated, resulting in a weak interaction with the soft FM particles. This is clearly seen in the cooling field dependence of H_{EB} and M_{EB} curves (inset of Fig. 5), the H_{EB} increases for the 20 kOe curve before it starts decreasing for higher fields. The decrease in H_{EB} for higher cooling fields is mainly due to the increase in the magnetization of the soft FM particles. It may also be noted that in $x=0$ at $T=3$ K [both in Fig. 5 and Fig. 3(a)], the $M(H)$ curve in the field increasing path follows a

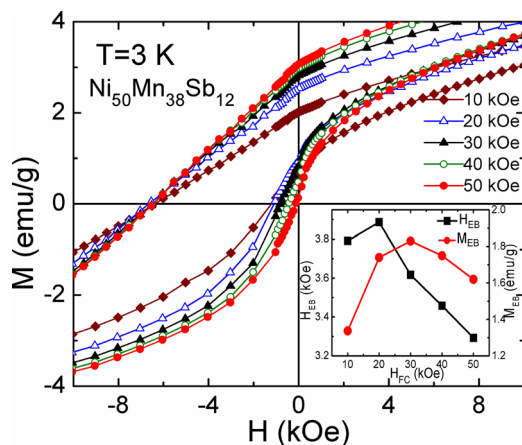


FIG. 5. (Color online) Magnetization isotherms measured at 3 K after field cooling the sample in different fields. The inset shows the cooling field dependence of H_{EB} and M_{EB} at 3 K.

non pinning loop, while it shows a pinned loop for the field decreasing path. This difference is due to the absolute shift in the FC $M(H)$ loop in negative field direction due to strong exchange coupling between the soft and hard particles at $T=3$ K for $x=5$. However, at higher temperatures (Fig. 3), the $M(H)$ loops show the pinning effect in both the field increasing and decreasing paths. This difference is due to the decrease in the exchange coupling between the soft and hard particles with temperature. This is clearly supported by the fact that the ZFC $M(H)$ loop at 3 K shows pinning effect in both the field paths [inset of Fig. 3(a)]. It is also of interest to note that in the case of $x=5$, the FC loops are pinned for both increasing and decreasing field paths even at 3 K, unlike the case of $x=0$. This again is reflective of the fact that the exchange bias is lower in $x=5$ as compared to that of $x=0$.

In conclusion, we have studied the effect of size reduction on the structural, magnetic and exchange bias behavior of $Ni_{50-x}Co_xMn_{38}Sb_{12}$ ($x=0$ and 5) ball milled samples. The reduction in the grain size significantly changes the structural as well as the magnetic properties of the ball milled samples as compared to their bulk counterparts. A large exchange bias behavior is observed in these samples, which is attributed to the increased magnetic anisotropy due to the decrease in the grain size. The present study is of importance in establishing structure-magnetic property correlations in similar multifunctional Heusler alloys.

¹K. Ullakko, J. K. Huang, C. Kantner, R. C. O'Handley, and V. V. Kokorin, *Appl. Phys. Lett.* **69**, 1966 (1996).

²R. Kainuma, Y. Imano, W. Ito, H. Morito, Y. Sutou, K. Oikawa, A. Fujita, K. Ishida, S. Okamoto, O. Kitakami, and T. Kanomata, *Appl. Phys. Lett.* **88**, 192513 (2006).

³T. Krenke, E. Duman, M. Acet, E. F. Wassermann, X. Moya, L. Mañosa, and A. Planes, *Nature Mater.* **4**, 450 (2005).

⁴A. K. Nayak, K. G. Suresh, and A. K. Nigam, *Appl. Phys. Lett.* **96**, 112503 (2010).

⁵V. K. Sharma, M. K. Chattopadhyay, K. H. B. Shaeb, A. Chouhan, and S. B. Roy, *Appl. Phys. Lett.* **89**, 222509 (2006).

⁶M. Khan, I. Dubenko, S. Stadler, and N. Ali, *Appl. Phys. Lett.* **91**, 072510 (2007).

⁷H. C. Xuan, Q. Q. Cao, C. L. Zhang, S. C. Ma, S. Y. Chen, D. H. Wang, and Y. W. Du, *Appl. Phys. Lett.* **96**, 202502 (2010).

⁸A. K. Nayak, K. G. Suresh, A. K. Nigam, A. A. Coelho, and S. Gama, *J. Appl. Phys.* **106**, 053901 (2009).

⁹A. K. Nayak, K. G. Suresh, and A. K. Nigam, *Acta Mater.* **59**, 3304 (2011).

¹⁰Q. Meng, Y. Rong, and T. Y. Hsu, *Phys. Rev. B* **65**, 174118 (2002).

¹¹Y. D. Wang, Y. Ren, Z. H. Nie, D. M. Liu, L. Zuo, H. Choo, H. Li, P. K. Liaw, J. Q. Yan, R. J. McQueeney, J. W. Richardson, and A. Huq, *J. Appl. Phys.* **101**, 063530 (2007).

¹²B. Tian, F. Chen, Y. Liu, and Y. F. Zheng, *Mater. Lett.* **62**, 2851 (2008).

¹³A. L. Alves, E. C. Passamani, V. P. Nascimento, A. Y. Takeuchi, and C. Larica, *J. Phys. D: Appl. Phys.* **43**, 345001 (2010).

¹⁴A. K. Nayak, K. G. Suresh, and A. K. Nigam, *J. Phys. D: Appl. Phys.* **42**, 115004 (2009).

¹⁵M. Gateshki, V. Petkov, G. Williams, S. K. Pradhan, and Y. Ren, *Phys. Rev. B* **71**, 224107 (2005).

¹⁶P. M. Shand, C. C. Stark, D. Williams, M. A. Morales, T. M. Pekarek, and D. L. Leslie-Pelecky, *J. Appl. Phys.* **97**, 10J505 (2005).

¹⁷K. Younsi, V. Russier, and L. Bessais, *J. Appl. Phys.* **107**, 083916 (2010).

¹⁸S. El-Khatib, S. Bose, C. He, J. Kuplic, M. Laver, J. A. Borchers, Q. Huang, J. W. Lynn, J. F. Mitchell, and C. Leighton, *Phys. Rev. B* **82**, 100411 (2010).

¹⁹T. Ichitubo, S. Takashima, E. Matsubara, Y. Tamada, and T. Ono, *Appl. Phys. Lett.* **97**, 182508 (2010).

²⁰E. E. Fullerton, J. S. Jiang, and S. D. Bader, *J. Magn. Magn. Mater.* **200**, 392 (1999).

²¹C. Binek, S. Polisetty, X. He, and A. Berger, *Phys. Rev. Lett.* **96**, 067201 (2006).